-RESEARCH PAPER-

International Journal of Mining and Geo-Engineering

IJMGE

IJMGE 58-4 (2024) 371-381

DOI: 10.22059/IJMGE.2024.367652.595118

Characterization and beneficiation potential for valuable heavy minerals from the Wadi Ibib stream sediments, southern coast of the Red Sea, Egypt

M. M. Fawzy [a,*], M. Bayoumi [a], H. Shahin [a], B. Emad [a], A. M. El Shafey [a], M. A. Abdel Azeem[a], A. M. Ismail [a], M. Diab [a]

[a] *Nuclear Materials Authority, Maadi, Cairo, Egypt.*

Article History:

Received: 04 November 2023.
Revised: 11 May 2024.
Accepted: 26 September 2024.

ABSTRACT

Economic heavy minerals (EHMs) in the Quaternary Stream Sediments of the Wadi Ibib were characterized mineralogically and chemically via optical microscopy, grain size distribution analysis, heavy liquid separation, X-ray diffraction (XRD), energy-dispersive X-ray fluorescence (EDXRF), and scanning electron microscopy (SEM). Information gathered from characterization studies confirmed that the heavy mineral content (specific gravity of more than 2.89) in the Ibib samples ranged between 8.18 and 17.52% by mass with an average of about 12.56% by mass. EDXRF data analyses also manifested that the content of ilmenite in the Ibib sample reached 0.2%, zircon 0.08%, rutile 0.07%, leucoxene 0.06%, almandine garnet 0.022%, cassiterite 0.007%, xenotime 0.006%, monazite 0.0008%, and magnetite was about 0.29% with high proportion of heavy silicates. With regard to raising the grade of the EHMs, heavy mineral concentrate was obtained through a rougher step on Wilfley Shaking Table No. 13, and then it was followed by two scavenging steps for the highest recovery obtained. The gravimetric concentration steps succeeded in raising the heavy mineral assay from 12.17% to 53.41% with a recovery of 80.42% in a yield of 20.38%. Finally, magnetic separation operations were conducted via low- and high-intensity magnetic separators at different intensities in an attempt to separate and obtain clean concentrates of EHMs that were ready for use in various modern technology industries.

Keywords: *Economic heavy minerals; Mineral beneficiation; Gravity concentration, Magnetic separation, Stream sediments; Southern coast of the Red Sea.*

1. Introduction

Placer deposits are a source of various mineral commodities, such as ilmenite, rutile, leucoxene, zircon, monazite, etc... [1,2]. These minerals and their metal-constituent products are the basic building blocks of modern developed industries. To ensure continuous and dynamic growth in this field, there is an increasing need to produce final concentrates with added value [3-7]. The Red Sea coast extends for hundreds of kilometers in Egypt and is considered one of the most promising coastal deposits for economic heavy minerals (HMs). Its importance appears as a source of rutile, ilmenite, zircon, and other economic minerals that are involved in high-tech industries all over the world. Therefore, the Nuclear Materials Authority conducted many studies related to the geological, mineralogical, mineral evaluation, radiological risks, and physical beneficiation of these placer deposits in order to assess the economic feasibility of exploitation [8-11].

Without a doubt, exploiting heavy mineral sand is easier and less expensive in mining and processing than other commodities [12]. Generally, HM sand deposits are massive and close to the surface, which facilitates simple exploration techniques and open-cast excavation [13]. Moreover, heavy mineral processing plants are currently well-established with considerable separation efficiency [14].

Physical separation of economic heavy minerals from the most common associated gangue in placer deposits is usually carried out by exploiting their differences in specific gravity, magnetic and electrostatic susceptibilities, and size-shape. Therefore, heavy minerals are concentrated and separated via physical techniques; first involving gravitational concentration, followed by the combination of magnetic and electrostatic separation [15-18] [9,10]. Flotation technology can be used as a supplementary separation stage in an effort to achieve a cleaner product [19-24].

The main subjects of this study are: (i) to clarify the physical, chemical, and mineralogical characterization for the Wadi Ibib stream sediments in order to find out the grain size distribution, apparent density, chemical composition, and finally the content, distribution, and confirmation of the economic heavy mineral; (ii) to conduct physical beneficiation tests on the Ibib sediments in order to recover the economic heavy minerals; and finally (iii) to characterize the separated products.

2. Experimental

2.1. Location and sampling

The Wadi Ibib area is located about 50 km south of Shalateen city, forming a vast area of sand and placer deposits. It lies in the northern

* Corresponding author: *E-mail address:* mm1_fawzy@yahoo.com (M.- M. Fawzy).

part of the Neoproterozoic Hamshana shear zone between latitudes of 22° 30' and 22° 46' N, and longitudes of 35° 26' and 36° 00' E (Fig. 1). The study area exhibits different rock units, such as ultramafics, metavolcanics and granites. The ultramafic rocks include serpentinite and gabbro. Metavolcanics in the Wadi Ibib area show two verities; basic and acidic metavolcanics that are intruding the metagabbro and metasedimentary rocks with sharp contact. Granites are represented by tonalite-granodiorite and biotite-muscovite granite. The investigated Quaternary deposits include gravel terraces, sabkha deposits, sand sheets, and wadi deposits (Fig. 1). A total of 12 stream sediment samples were collected through pits arranged in one profile in the middle of the Wadi Ibib. The pits are about 50cm in diameter, 70 -100 cm in depth, and 2-6 km apart. In the field, each pit sample was mixed well to form a homogeneous sample in order to be ready for various investigations in the lab.

Physical and chemical characterization in addition to mineralogical investigation and physical upgradability processes was conducted on each collected sample from 12 samples, besides a representative sample, that was prepared by taking an equal amount of each sample and mixing them well to form the Ibib representative sample (Ibib $_{rep.}$).

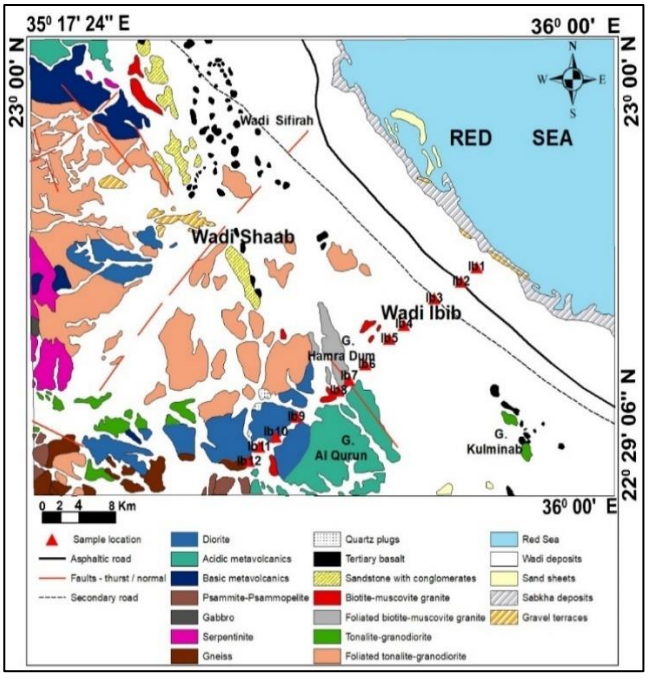

Fig. 1 (A) The general location map of the Wadi Ibib area, (B) The geological map showing sampling locations of the Wadi Ibib area, south Eastern Desert of Egypt (Modified after [8]).

2.2. Sample Characterization

2.2.1. Grain Size distribution analyses

Grain size distribution analyses for the Wadi Ibib stream sediments samples were performed using a mechanical sieve shaker with a set of sieves with aperture diameters of 2.0, 1.0, 0.5, 0.250, 0.125, and 0.063 mm (ASTM codes) for 15 minutes. All size fractions were weighed and their distributions recorded.

2.2.2. Apparent Density measurements

The apparent density was measured for each sample by weighing the sample and pouring it inside a graduated cylinder, then it was compacted well. The density values were obtained from dividing the mass of the sample by its volume.

2.2.3. Heavy mineral content determination

For determining the heavy mineral content of the Ibib samples, approximately 50g of each sample was separated via heavy liquid separation test using bromoform ($CHBr_3$) with a specific gravity of 2.89. The heavy and light mineral fractions were washed with acetone, dried, and finally weighed to determine the heavy mineral content in each sample.

2.2.4. Mineral Identification

The mineralogical identification was carried out via an X-ray diffraction (XRD) instrument along with an environmental scanning electron microscope (SEM) (Philips Model XL 30) equipped with an energy dispersive spectrometer (EDS) unit. Heavy mineral fractions were separated through magnetic fractionation using a Carpco high intensity magnetic separator (HIMS) which divided each sample into four magnetic (mag.) fractions at 0.04A, 0.8A, 1.5A, 2.5A as well as a non-magnetic (non-mag.) fraction. An Olympus stereo binocular microscope was also used to prepare and select pure mineral grains by hand picking for XRD and SEM analyses.

2.2.5. Quantification of Heavy minerals

X-ray fluorescence spectroscopy (XRF) is one of the most convenient and rapid analytical techniques for determining chemical assays of solid samples, so it is the most suitable technique in the field of physical beneficiation [26, 27]. The estimation of heavy mineral content in a representative Ibib sand sample was conducted using chemical assays on magnetically separated subsamples via an energy-dispersive X-ray fluorescence (EDXRF) Rigaku spectrometer with polarized optics. This method was attempted by [28] and developed by [29] who demonstrated that it is a relatively simple, rapid, low-cost, non-toxic, and eye-strain-free method compared to the microscopic grain counting technique. This method was implemented through the following steps: (1) about 100-150 grams of Ibib representative sample were prepared by blending equal proportions of 12 samples under investigation, (2) sieving was done using a 1mm sieve, (3) attrition using hydrogen peroxide was performed on a -1mm fraction, (4) magnetite separation was carried out using a hand magnet, (5) EDXRF spectrometric analyses were implemented on a part of the magnetite-free sample, (6) magnetic separation via HIMS was performed on the remaining part of the sample into four fractions that are magnetic at 0.8, 1.5, and 2.5A and non-magnetic at 2.5A, (7) EDXRF analyses of these fractions for the elemental oxides in the formula of heavy minerals, and (8) computation of the contents of heavy minerals assuming their stoichiometric composition. The schematic flow-sheet of heavy mineral estimation using EDXRF spectrometry is depicted at Figure 2.

2.3. Sample Beneficiation

The beneficiation experiments were carried out on a representative sample weighing about 20 to 25 kg. Firstly, the total heavy mineral concentration process was conducted via wet-gravity concentration using a Wilfley shaking table No. 13 for get rid of the most common associated light gangue minerals as much as possible. After the completion of each concentration stage (rougher and scavenger), a 100 g representative sample of each of the gravity concentration products (concentrate and tail) was subjected to bromoform separation for the determination of the THM assay. The obtained heavy tabling concentrates were firstly separated using a low-intensity magnetic separator (LIMS) to separate magnetite. Free-magnetite mineral fractions were subjected to Carpco dry high-intensity magnetic separator (DHIMS) Model MLH (13) III-5" 15 to separate paramagnetic from diamagnetic minerals and obtain a clean concentrate from theses fractions. The magnetic separation processes via DHIMS were achieved at pre-optimized factors of a medium air gap of 1.5 cm, magnetic field current at 0.8, 1.5 and 2.5A, magnetic roll speed 30 rpm and an optimum feed rate of 39.2 g/min.

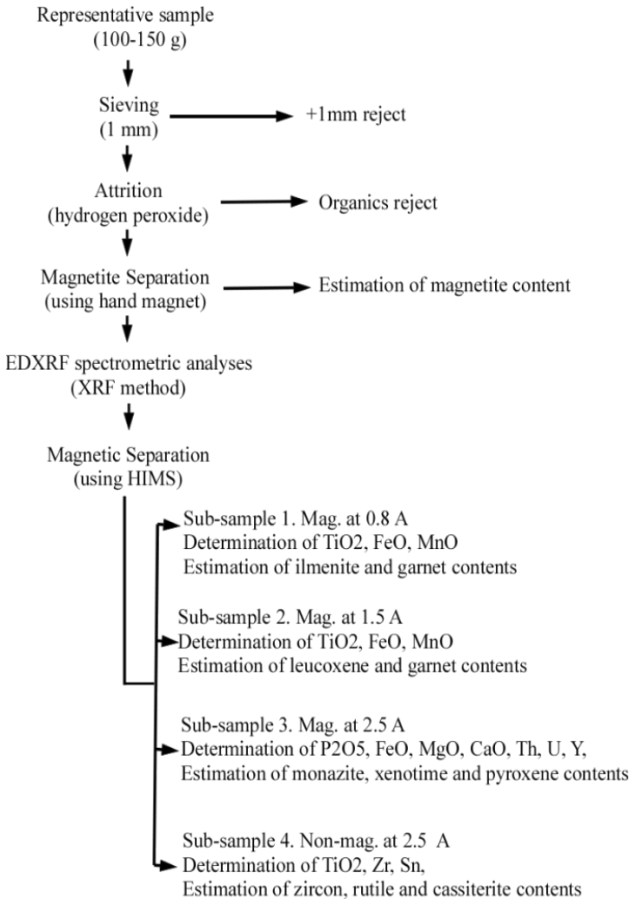

Fig. 2 The schematic flow-sheet of heavy mineral estimation using energy-dispersive X-ray fluorescence (EDXRF) spectrometry.

3. Results and Discussion

3.1. Ibib sample characterization results

The EDXRF analyses for Ibib head sample are shown in Table (1). The head assays of the main oxides showed contents of 3.57% of Fe_2O_3 and 0.49% for TiO_2. The highest trace elements were zirconium (329 ppm), Cr (300 ppm), Co (169 ppm), and Ni (116 ppm), while Zn, Y, Pb, Cu, Nb, and Sn showed low contents.

Grain size distribution is one of the most important physical parameters of heavy mineral sand, as it has a significant impact on the separation efficiency using different physical separation processes. Many research papers have confirmed that the highest percentage of liberated heavy minerals was found in the size fraction of less than 250 µm [30]. Grain size distribution analyzes of the Wadi Ibib samples are presented in histograms in Figure 3. The results showed a high degree of homogeneity for the samples and from the mean values for the size distribution, it also confirmed that the highest percentage (85.30% mass) of size retained in a range from 1 to 0.063 mm, while the gravel and very coarse sand fractions were about 12.29% mass, and the silty size fraction was calculated as 2.42% mass. For $Ibib_{rep.}$, it was 87.57% mass for size range of 1-0.063mm, 10.72% mass for the gravel and very coarse sand fraction, and 1.70% mass for the silty size fraction.

The values of the apparent density measurements were used as evidence for the presence of heavy mineral concentrations in the studied samples, in addition to using these values to estimate the reserves of heavy minerals in the area under investigation [8-10]. As for the apparent density measurements of the Wadi Ibib samples which are shown in Figure 4, the values ranged from 1.64 to 1.93 g/cm^3, with an average of about 1.79 g/cm^3 and the value of the Ibib representative sample was 1.81 g/cm^3. Compared to the typical values of dry density for normal sand which are estimated at 1.5 g/cm^3 [31], this indicates that heavy minerals were occurred in high concentrations. The heavy mineral content in each sample was determined and separated by the heavy liquid separation technique using bromoform and the results are presented in Figure 4. The results confirmed that the total heavy mineral content in the Ibib samples ranged between 8.18 and 17.52% mass with an average of about 12.56% mass and 12.17% mass for $Ibib_{rep.}$.

Table 1. The EDXRF analyses of the Ibib head bulk samples.

Major Oxides (%)						Elements (ppm)										
Fe_2O_3	CaO	TiO_2	P_2O_5	K_2O	MnO	Zr	Cr	Ni	Co	V	Zn	Y	Pb	Cu	Nb	Sn
3.57	3.17	0.49	0.079	0.85	0.077	329	300	116	169	158	70	27	13.8	34.7	10	57

Heavy mineral (HM) size distribution analysis for the studied samples was performed and depicted at Figure 5. The mean results for 12 samples concluded that 96.44% mass of the HMs retained in the size range of 1 to 0.063 mm while, zero percent of HMs was in the size fraction greater than 1mm and 3.57% mass of HMs was presented in the silt size fraction (-0.063mm). The results for a representative Ibib sample were as follows: 96.29% mass of HMs was kept in the size fraction of -1+0.063 mm, 0% mass in the +1mm size fraction, and 3.71% mass of the HMs in silty fraction.

Microscopic examination using the Stereo-binocular microscope and SEM analyses which were supplied with an EDS unit for the heavy mineral fractions obtained from bromoform separation revealed the presence of a large group of economic heavy minerals distributed in most size fractions, but more concentrated in the fine ones, less than 0.25 mm. They were shown as follows: ilmenite (Fig. 6a), leucoxene (Fig. 6b), almandine garnet (Fig. 6c), sphene (Fig. 6d), rutile (Fig. 7a), zircon (Fig. 7b), Cu-Zn mineral (Fig. 7c), cassiterite (Fig. 7d), xenotime (Fig. 8a), monazite (Figs. 8b and c), and gold (Fig. 8d).

For detailed mineralogical study, the magnetic fractionation of heavy bromoform fractions was conducted using a Carpco high-intensity magnetic separator (HIMS). Each heavy bromoform sample was magnetically separated into five fractions (magnetic at 0.04A, magnetic at 0.8A, magnetic at 1.5A, magnetic at 2.5A, and non-magnetic at 3A). Each fraction was weighted and calculated with respect to the percentage of heavy minerals and the results are presented in Figure 9.

Magnetic fractionation process of the Ibib samples manifested that the magnetic fraction at 1.5A represents the highest value ranging from 37.67 to 64.15% mass with an average of about 48.78% mass, followed by the magnetic fraction at 3A where the values ranged between 7.16 to 29.33% mass with an average of 18.85% mass. Meanwhile the non-magnetic fraction at 3A had values between 12.93 to 22.7% mass with an average of 15.73. The magnetic fraction at 0.8A ranged between 1.6 to 27.62% mass with an average of 13.92% mass. As for the lowest value of magnetic fractionation, it had a magnetic fraction of 0.04A which ranged from 1.14 to 4.15% mass with an average of 2.72% mass. With regard to the Ibib representative sample ($Ibib_{rep.}$), the magnetic fractionation results were close to the average values of the samples and their results are as follows: 57.63% mass for the magnetic fraction at 1.5A, 18.53% mass for the magnetic fraction at 2.5A, 13.90% mass for the non-magnetic fraction at 2.5A, 7.08% mass for the magnetic fraction at 0.8A, and 2.86% mass for the magnetic fraction at 0.04A (Figure 9).

The mineralogical confirmation of the magnetic fractionation of the Wadi Ibib representative sample was conducted via XRD analyses and the diffractograms for the various fractions are depicted in Figures 10 and 11. Figure 10a showed that the magnetic fraction at 0.04 amps contained mainly magnetite and hematite which had ASTM Card No.

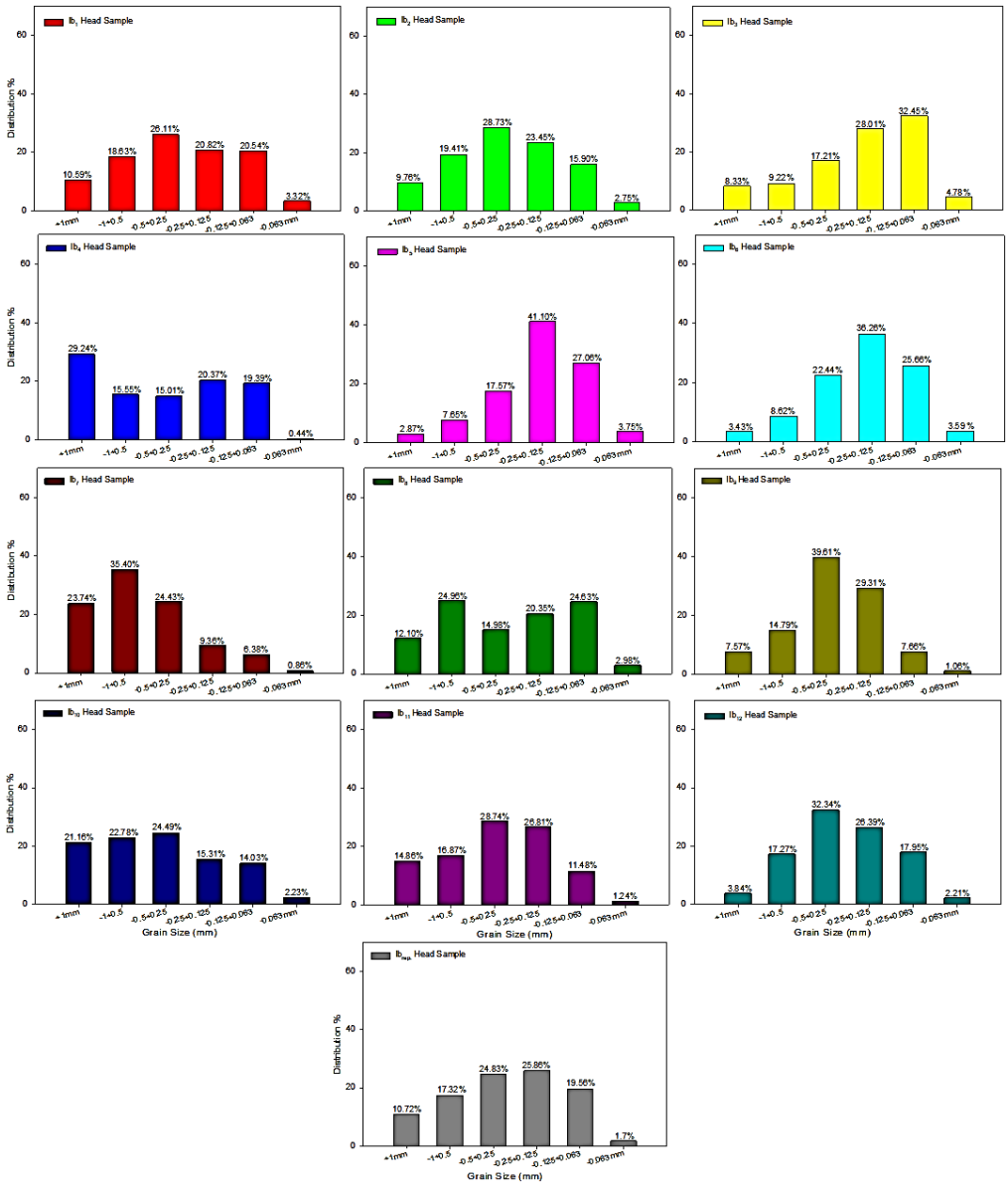

Fig. 3 Histograms showing the grain size distribution analyses for the Ibib stream sediments samples.

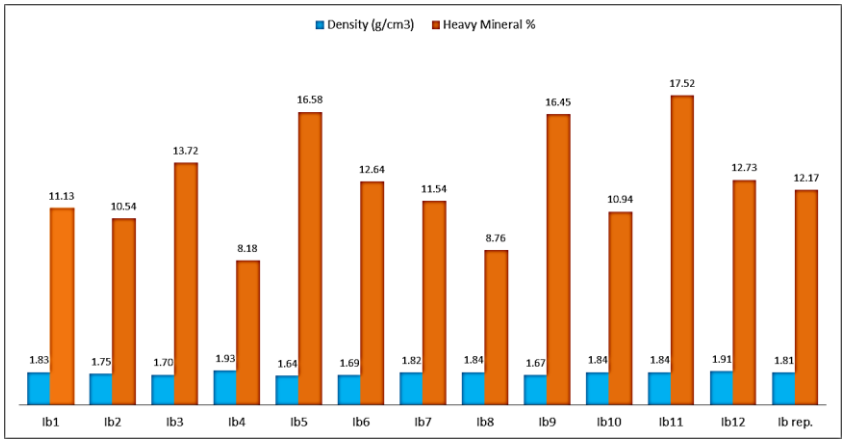

Fig. 4 Apparent density measurements and heavy mineral content in the Wadi Ibib stream sediment samples.

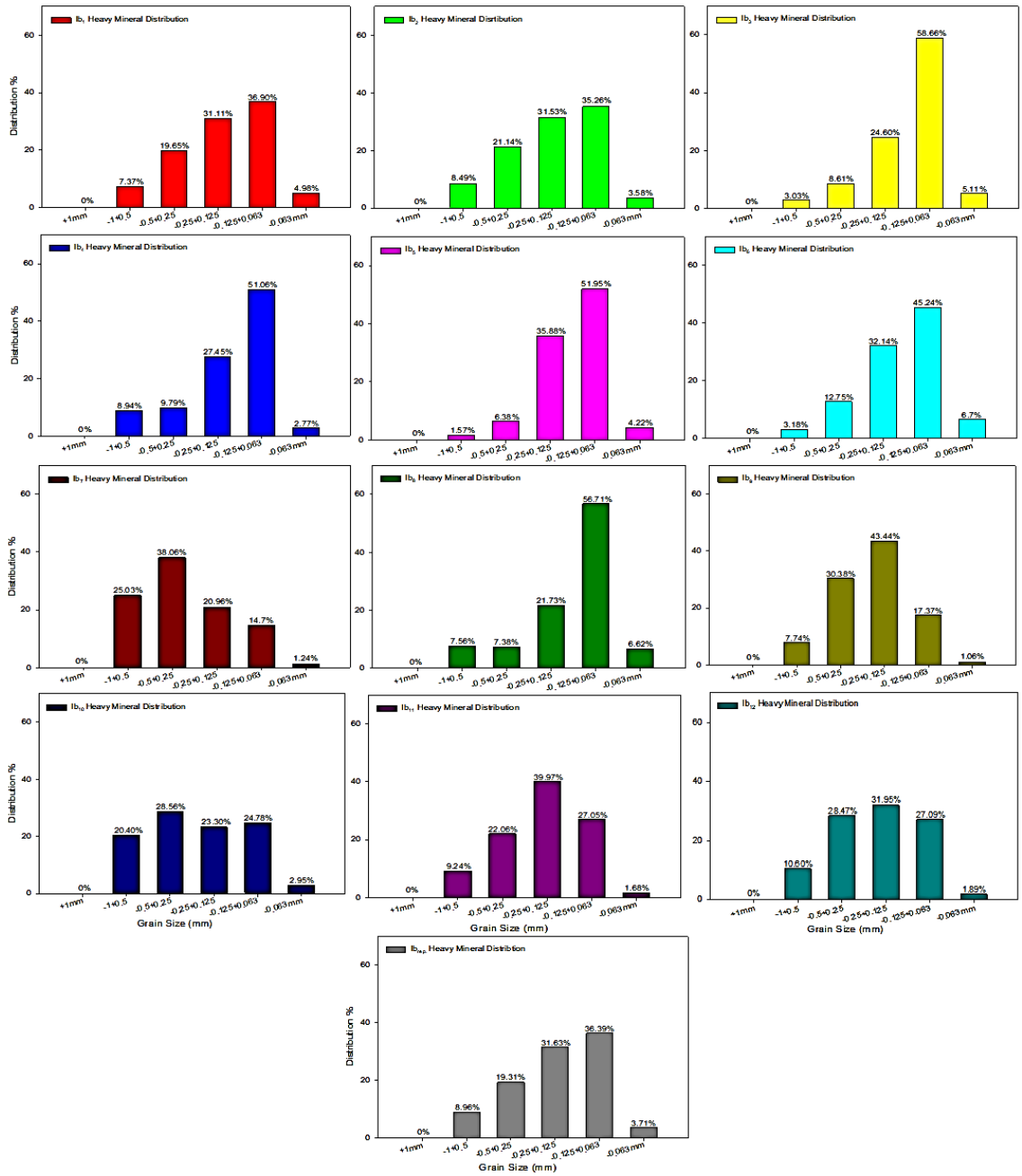

Fig. 5 Histograms showing the heavy minerals size distribution analyses for the Ibib samples.

76-1849 and 58-599, respectively. Meanwhile the magnetic fraction at 0.8 amps was mainly composed of ilmenite and actinolite which had ASTM Card No. 03-778 and 85-2157, respectively (Figure 10b). The alteration products of ilmenite (leucoxene), actinolite, and almandine separated as the magnetic fraction at 1.5 amps had ASTM Card No. 03-778, 85-2157 and 74-1553, respectively (Fig. 10c).

Magnetic separation at 2.5 amps proved the presence of rutile, epidote, actinolite, and monazite which had ASTM Card No. 88-1175, 17-514, 85-2157, and 46-1295, respectively (Fig. 11a). Meanwhile the non-magnetic fraction at the same amperes showed the presence of rutile, cassiterite, zircon, quartz, and diopside which had ASTM Card No. 72-1148, 14-567, 06-266, 85-798, and 83-98, respectively (Fig. 11b).

The results of processing and magnetic fractionation for the Ibib head representative sample for the quantification of heavy minerals using a hand magnet and HIMS indicated that the oversize fraction (+1mm) represents about 11.88% while the slime after attrition represents 6.92%. The hand magnet separated fraction was about 0.29%, the magnetic fraction at 0.8A was about 8.63%, magnetic fraction at 1.5A was about 5.42%, and magnetic fraction at 2.5A was 3.21%, while the non-magnetic fraction at 2.5A represented about 63.65%.

The EDXRF analyses for the major oxides and trace elements of different magnetic fractions for the Ibib head sample are shown in Table (2). The data from analyses, as well as the magnetic fractionation results used to compute the contents of heavy minerals assuming their stoichiometric composition revealed that the content of ilmenite in the representative sample reached 0.2%, zircon was 0.08%, rutile was 0.07%, leucoxene was 0.06%, almandine garnet was 0.022%, cassiterite was 0.007%, xenotime was 0.006%, monazite was 0.0008%, and magnetite was about 0.29%.

3.2. Beneficiation results

Beneficiation of the Ibib samples with the aim of raising the grade of

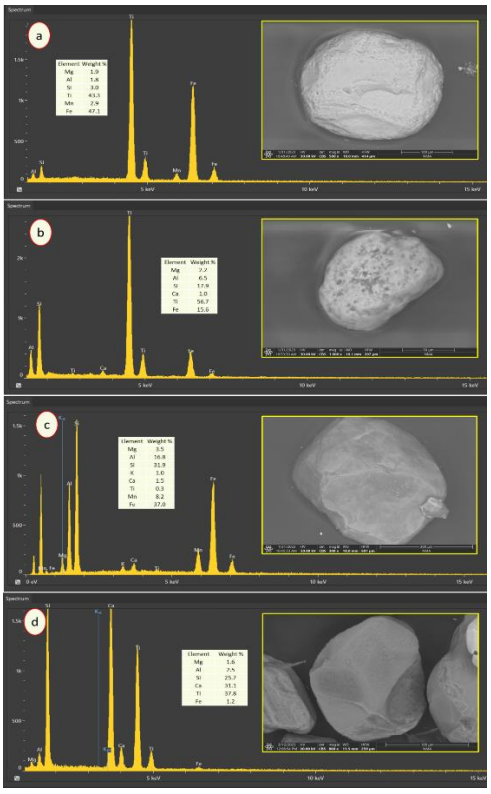

Fig. 6 Back-scattered electron (BSE) images and corresponding EDS spectra for ilmenite (a), leucoxene (b), almandine (c), and sphene (d).

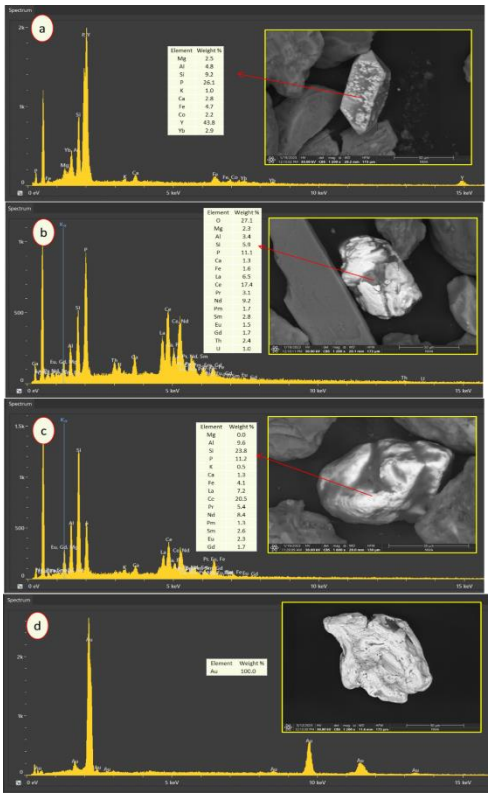

Fig. 8 BSE images and corresponding EDS spectra for xenotime (a), monazite (b) and (c), and gold (d).

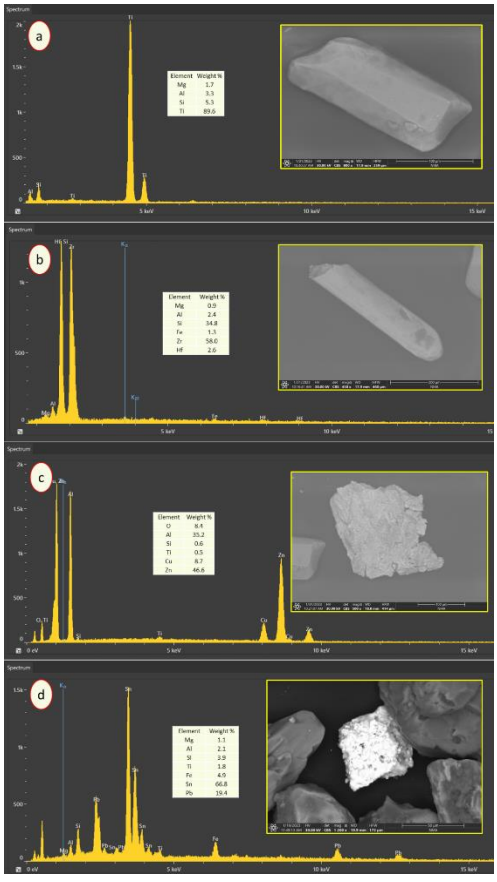

Fig. 7 BSE images and corresponding EDS spectra for rutile (a), zircon (b), Cu-Zn mineral (c), and cassiterite (d).

economic heavy minerals was conducted via gravity concentration processes using a shaking table in order to eliminate low-density gangue silicate minerals, such as quartz and feldspar which were present in large proportions and produced a heavy mineral concentrate portion. Meanwhile, the magnetic fractionation process was carried out on the heavy portion in order to separate the magnetic heavy minerals from the paramagnetic minerals and also from the diamagnetic minerals.

3.2.1. Shaking table concentration

Wilfely Shaking Table No. 13 was used as equipment for raising the grade of the heavy minerals by going through two rounds of scavenging concentration stages after a rougher step to recover the remaining heavy minerals in tails that were not recovered during the initial roughing stage.

After several tests were conducted on the shaking table to improve the separation conditions, it became clear that the optimal operating conditions for the roughing stage are a 134 g/min feed rate, 14 l/min water flow rate, 1.5cm stroke length, and a 9° inclination angle. Meanwhile the best operating conditions for the scavenging stages were 140 g/min feed rate, 17.5 l/min water flow rate, 2 cm stroke length, and an 11° inclination angle. It is quite obvious that the scavenging stages had values for operating conditions that were greater than those of the roughing stage and this is due to an increase in the light gangue mineral percentage and a decrease in the heavy minerals during the scavenging stages compared to the roughing stage. After completing the stages of gravity concentration (rougher and scavenger) for the sample, a representative sample weighting about 100 g from each fraction of the products (concentrate and tail) was subjected to a heavy-liquid separation test using bromoform in order to determine the assay of heavy minerals and calculate the material balance. The results are presented in Table 3. The results showed that the scavenging process is very important and effective, because it raised the recovery rate from 61.73% in the rougher stage to 80.42% after the scavenging stages.

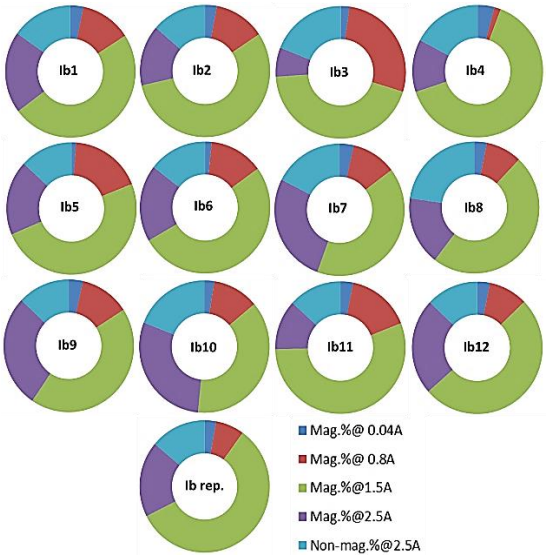

Fig. 9 Magnetic fractionation content of heavy minerals in the Ibib samples via DHIMS.

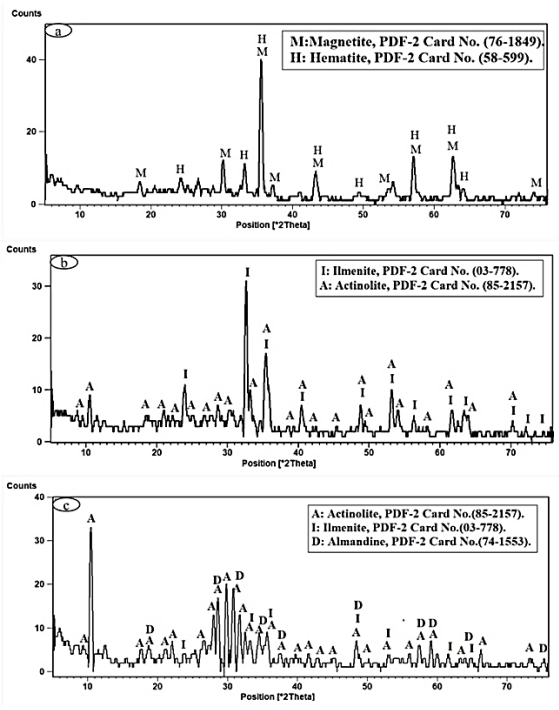

Fig. 10 XRD diffractograms showing: (a) magnetite and hematite separated as the magnetic fraction at 0.04 amps, (b) ilmenite and actinolite separated as the magnetic fraction at 0.8 amps, (c) almandine, ilmenite, and actinolite separated as the magnetic fraction at 1.5 amps of the Wadi Ibib representative sample.

The EDXRF spectrometric analysis for the final concentrate was displayed against the head sample analysis in Table 4 that also showed the enrichment ratio values. These values were calculated by dividing the grade of concentrate by the grade of the feed (c/f) and they indicated how many times the concentrate's element concentration was relative to the feed. The enrichment ratio values for major elements, such as Fe_2O_3 and TiO_2 showed a clear improvement and increased by 2.073% for Fe_2O_3 and 2.63 for TiO_2. As for the trace elements, such as Zr, Cr, Co, Y, U, and Th, they showed high values for the enrichment ratio in the concentrate compared to the feed sample. This is the results of doubling of the contents of minerals, such as ilmenite, magnetite, rutile, sphene, zircon, almandine, monazite, and xenotime in the concentrate.

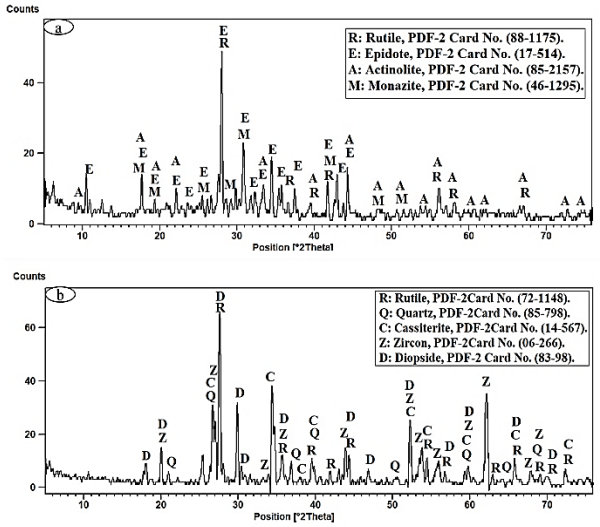

Fig. 11 XRD diffractograms showing: (a) Rutile, epidote, actinolite and monazite separated as the magnetic fraction at 2.5 amps, (b) rutile, zircon, cassiterite, diopside and quartz separated as the non-magnetic fraction at 2.5 amps of the Wadi Ibib representative sample.

Table 2. EDXRF analyses results of the Ibib head sample and their different magnetic fractions

Elemental oxides	Mag. @0.8A	Mag. @1.5A	Mag. @2.5A	Non. @2.5A
Fe2O3	11.2	10.4	5.54	0.772
CaO	4.03	5.8	4.32	2.62
TiO2	1.52	0.878	0.635	0.128
P2O5	0.083	0.095	0.084	0.085
K2O	0.624	0.768	0.634	0.916
MnO	0.22	0.213	0.106	0.022
Cr	970	630	345	40
Ni	380	280	229	42
Co	380	330	223	33
V	290	374	252	57
Zn	215	180	103	37
Y	46	54	48	16
Pb	18.5	17.6	17.4	11.5
Cu	150	111	59.8	22
Th	<0.1	<0.1	14.6	<0.1
U	<0.1	<0.1	<0.1	<0.1

3.2.2. Magnetic separation

The heavy mineral fractions were used as feed for a low-intensity magnetic separator (LIMS) for the separation of magnetite as a ferromagnetic mineral fraction and the non-magnetic fraction were subjected to the Carpco high intensity magnetic separator (HIMS) Model MLH (13) III-5" to fractionate free-magnetite mineral fraction into paramagnetic and diamagnetic fractions. Four magnetic fractions resulted: ferromagnetic mineral fraction, paramagnetic mineral fraction that separated at 0.8A, paramagnetic mineral fraction separated at 1.5A, and paramagnetic mineral fraction at 2.5A. The non-magnetic mineral fraction separated at 2.5A was also obtained.

3.2.2.1 Ferromagnetic mineral fraction

Magnetite is the separation product of this fraction using a low-intensity magnetic separator and it represents about 0.22% of the mass of the heavy mineral fraction. The magnetite fraction was confirmed by the SEM analyses where the back-scattered electron (BSE) image with the

Table 3. The material balance of the different products of the gravity concentration via shaking table for the Ibib stream sediments representative samples.

Products of tabling		Yield (%)	Heavy mineral assay (%)	Heavy mineral recovery (%)
Concentrate	Roughing stage	14.32	52.46	61.73
	Scavenging Round 1	3.18	40.03	10.45
	Scavenging Round 2	2.88	34.82	8.24
	Total	20.38	53.11	80.42
Tail	Total	79.62	2.99	19.58
Feed	Total	100	12.17	100

Table 4. The EDXRF analyses demonstrating the feed grade, concentrate grade and enrichment ratio (E.R.) for the Ibib technological samples as a results of gravity concentration via shaking table.

	Feed Grade	Concentrate Grade	Enrichment Ratio (E.R.)
		Major Oxides in %	
Fe_2O_3	3.57	7.4	2.07
CaO	3.17	4.95	1.56
TiO_2	0.49	1.29	2.63
P_2O_5	0.097	0.111	1.14
K_2O	0.85	0.632	0.74
MnO	0.077	0.152	1.97
		Trace Elements in ppm	
Cr	300	906	3.02
Zr	329	645	1.96
Ni	116	145	1.25
Co	169	234	1.38
V	158	329	2.08
Zn	70	111	1.59
Y	27	50	1.85
Pb	13.8	17.2	1.25
Cu	34.7	26	0.75
Th	<0.1	10.3	103
U	<0.1	<0.1	

corresponding energy dispersive spectrum (EDS) and its stereo microscopic image are shown at Figures 12a and b, respectively. The SEM data for magnetite as a separate grain is depicted in Figure 12c, in which the iron content was about 94.6%.

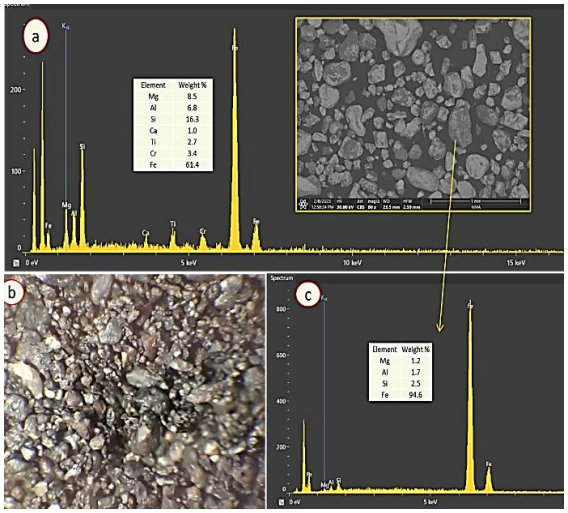

Fig. 12 Representative back-scattered electron (BSE) image with corresponding EDS spectra, and stereo microscopic image for magnetite fraction (a), (b) respectively, magnetite (c).

3.2.2.2. Magnetic fraction at 0.8 A

This fraction represents about 2.15% of the mass of the heavy mineral fraction. The BSE image and its corresponding EDS for this magnetic fraction are shown at Figure 13a and clarified that the main content was iron (41.6%), titanium (25.8%), silicon (16.4%), and manganese (2.1%); this means that ilmenite was the main separated mineral with the traces of almandine. The stereo microscopic image shown in Figure 13b also proved the presence of ilmenite as an essential mineral with almandine as traces. Ilmenite grain with an elemental composition of 50% Fe and 40.8% Ti is presented at Figure 13c.

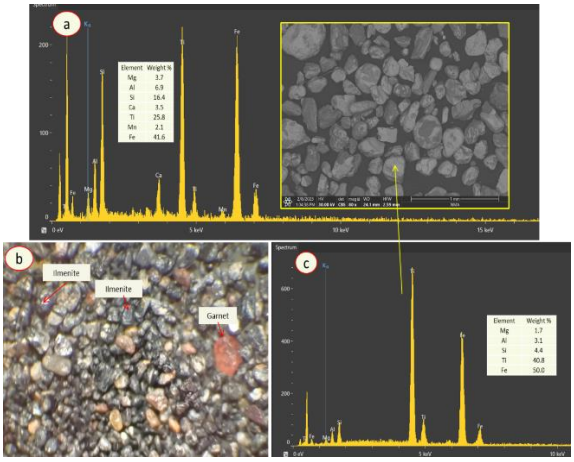

Fig.13 Representative BSE image with corresponding EDS spectra, and stereo microscopic image for magnetic fraction at 0.8A (a), (b) respectively, ilmenite (c).

3.2.2.4. Magnetic fraction at 1.5 A

This fraction represents about 4 % of the mass of the heavy fraction of the Ibib samples. The SEM data shown in Figure 14a as well as the stereo microscopic image shown in Figure 14b proved that the main elemental content was Si (35.1%). Fe (26.5%), Al (14.1%), Ca (12.3%), and Ti (6.8%) implying that heavy silicates, such as pyroxene, epidote, and amphiboles along with leucoxene and almandine were the main minerals that occurred. SEM data concerning almandine, pyroxene, and leucoxene content are shown in Figure 14c, d, and e, respectively.

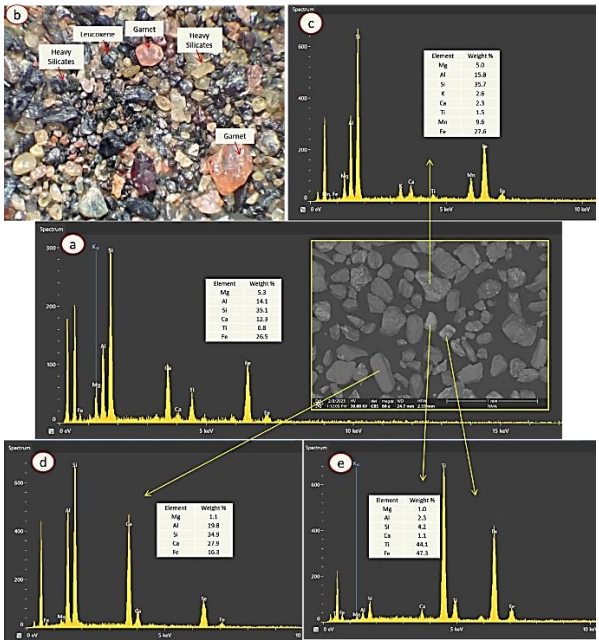

Fig.14 Representative BSE image with corresponding EDS spectra, and stereo microscopic image for magnetic fraction at 1.5A (a), (b) respectively, almandine (c), pyroxene (d), leucoxene (e).

3.2.2.4. Magnetic fraction at 2.5 A

The heavy fraction of the Ibib samples contains a 1.99% mass magnetic fraction at 2.5A. The SEM results (Fig. 15a) and stereo microscopic image (Figure 15b) proved that this fraction contained mainly heavy silicate minerals, in addition to the presence of monazite which is confirmed in Figure 15c.

3.2.2.5 Non-magnetic fraction at 2.5 A

The Ibib heavy fraction contains about 12.02% of the mass of the non-magnetic fraction at 2.5A. The SEM data in Figure 16a proved that the main elemental content was Ti (31.0%), Si (27.0%), Ca (19.5%), Zr (8.5%), and Hf (0.8%). The stereo microscopic image in Figure 16b as well as the SEM data in Figures 16c, d, e, and f confirmed that stistaite, sphene, rutile, and zircon were the main minerals in this fraction. A schematic sequence for processing and separating economic heavy minerals from the Ibib stream sediments sample is depicted as a flow sheet in Figure 17.

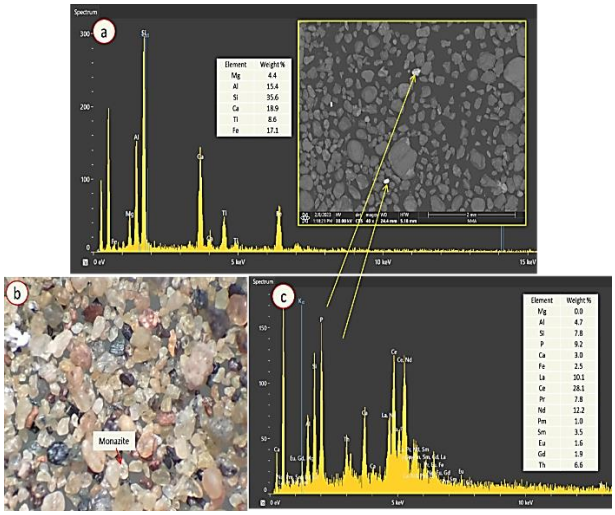

Fig.15 Representative BSE image with corresponding EDS spectra, and stereo microscopic image for magnetic fraction at 2.5A (a), (b) respectively; monazite (c).

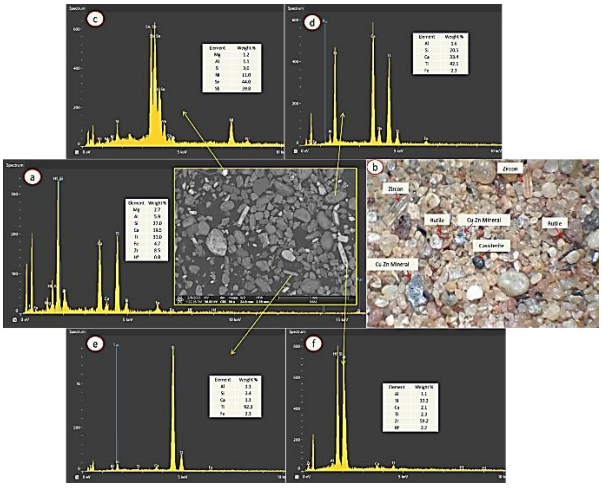

Fig. 16 Representative BSE image with corresponding EDS spectra, and stereo microscopic image for non- magnetic fraction at 2.5A (a), (b) respectively, stistaite (c), sphene (d), rutile (e), zircon (f).

4. Conclusion

The integration of the EDXRF analyzes data with the results of magnetic fractionation to calculate the content of heavy minerals in the Wadi Ibib area, assuming its stoichiometric composition resulted in the content of ilmenite reaching 0.2%, zircon 0.08%, rutile 0.07%, leucoxene 0.06%, almandine garnet 0.022%, cassiterite 0.007%, xenotime 0.006%, monazite 0.0008 %, and magnetite at about 0.29%.

As for the results of the different processes of physical upgrading, they showed that the gravity separation process succeeded in raising the heavy mineral assay from 12.17% in the head sample to 53.41% in the final concentrate with a yield of 20.38%. The scavenging stage also showed its importance and effectiveness, because it raised the recovery rate from 61.73 % for the roughing stage to 80.42% after the two rounds of scavenging stages. The final step to separate the different concentrates of economic minerals was carried out using a dry high-intensity magnetic separator from the Carpco at different current strengths (amps) to obtain clean heavy mineral concentrates, such as magnetite, ilmenite, leucoxene, rutile, and zircon.

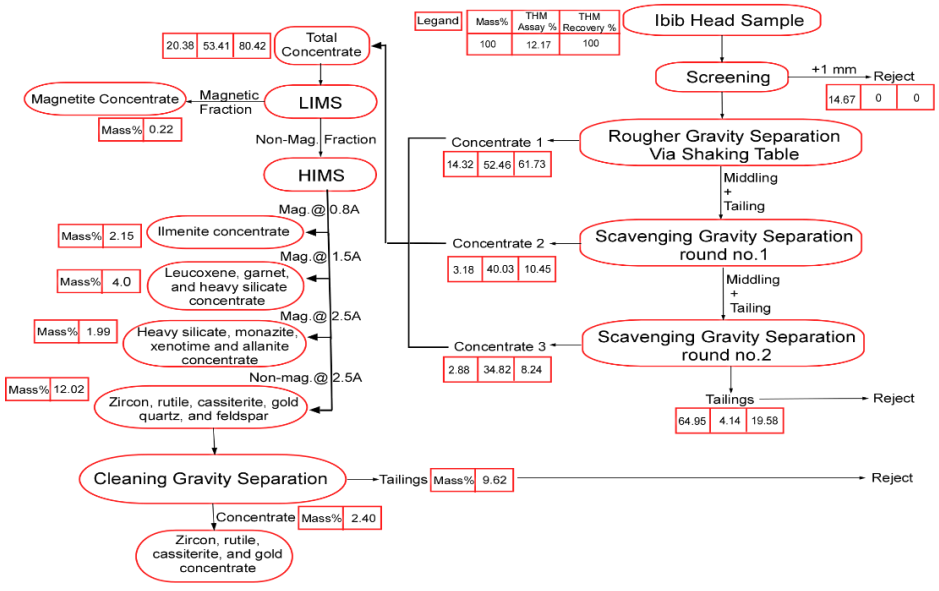

Fig. 17 Flow sheet with material balance for the recovery of economic heavy minerals from the Ibib head samples.

REFERENCES

[1] H. G. Dill, Heavy minerals from ore guide to the deposit. Applied Earth Science 125(2) (2016) 80–81. doi:10.1080/03717453.2016.1166622

[2] M. Dieye, M. Lichtervelde, A. Ndiaye, M. Gueye, S. Blancher, Mineralogical Characterization of Heavy Mineral Concentrates from Senegalese Great Cost by Using Qemscan and SEM. International Journal of Geosciences 11(2020) 800-817. doi: 10.4236/ijg.2020.1112041.

[3] M. Abdel-Aal, Abdel-Karim, M. Zaid, M. I. Moustafa, M. G. Barakat, Mineralogy, chemistry and radioactivity of the heavy minerals in the black sands, along the northern coast of Egypt. Journal of African Earth Sciences 123 (2016) 10-20, ISSN 1464-343X, https://doi.org/10.1016/j.jafrearsci.2016.07.005.

[4] A. Papadopoulos, I.T. Tzifas, H. Tsikos, The Potential for REE and Associated Critical Metals in Coastal Sand (Placer) Deposits of Greece: A Review. Minerals 9 (2019) 469. https://doi.org/10.3390/min9080469

[5] D. Singh, S. Basu, B.R. Mishra, Development of Flow Sheets to Recover Critical Minerals from Brahmagiri Lean-Grade Beach Sand Deposit'. J. Inst. Eng. India Ser. D (2023). https://doi.org/10.1007/s40033-023-00514-6

[6] S. Routray, R. Swain, R.B. Rao, A Study on Heavy Mineral Distribution Pattern Along Brahmagiri Coast of Odisha, India and Its Beneficiation to Recover Industrial Minerals. In: Pandey, P.M., Kumar, P., Sharma, V. (eds) Advances in Production and Industrial Engineering. Lecture Notes in Mechanical Engineering. Springer, Singapore (2021) https://doi.org/10.1007/978-981-15-5519-0_22

[7] A. Lakshmi Venkatesh, K.S.N. Reddy, K. Bangaku Naidu, C. Aruna, N. Ankita Varma, K. Sandeep Kumar, Heavy Minerals Studies of Coastal Sands from Bavanapadu to Kalingapatnam, Andhra Pradesh, East Coast of India. In: Jayaraju, N., Sreenivasulu, G., Madakka, M., Manjulatha, M. (eds) Coasts, Estuaries and Lakes. Springer, Cham. (2023) https://doi.org/10.1007/978-3-031-21644-2_11

[8] M. Fawzy, M. Abu El Ghar, M. Gaafar, I. El shafey, M. Diab, A. Hussein, Diit Quaternary Stream Sediments, Southern Coast of the Red Sea, Egypt: Potential Source of Ilmenite, Magnetite, Zircon, and Other Economic Heavy Minerals. Mining, Metallurgy & Exploration (2022a) 39:655–667.

[9] M. Fawzy, M. Abu El Ghar, M. Gaafar, I. El shafey, M. Diab, A. Hussein, Recovery of valuable heavy minerals via gravity and magnetic separation operations from Diit Quaternary stream sediments, southern coast of the Red Sea, Egypt. J. Phys.: Conf. Ser. 2305 012020 (2022b). doi:10.1088/1742-6596/2305/1/012020

[10] M. Diab, M. Abu El Ghar, M. Gaafar, A. El shafey, A. Hussein, M. Fawzy, Potentiality of Physical Upgrading for Valuable Heavy Minerals from Sermatai Area, Egypt. Journal of Mining and Environment (JME) 13(1) (2022) 15-32. DOI:10.22044/jme.2022.11479.2136

[11] I. Gaafar, M. Fawzy, M. Diab, M. Hanfi, Radiological Hazards Assessment of Stream sediments at Wadi Diit and Wadi Sermatai area, Southern Eastern Desert, Egypt. Journal of Radioanalytical and Nuclear Chemistry 331 (2022) 1795–1806 https://doi.org/10.1007/s10967-022-08247-8

[12] G. Jones, Mineral Sands: An Overview of the Industry; Iluka Company: Perth, Australia, (2008) p. 26.

[13] B. Gosen, D. Bleiwas, G. Bedinger, K. Ellefsen, A. Shah, Coastal deposits of heavy mineral sands: Global significance and US resources. Min. Eng. 68 (2016) 36–43.

[14] C. Caroline, Gonçalves, F. Paulo, Braga. Heavy Mineral Sands in Brazil: Deposits, Characteristics, and Extraction Potential of Selected Areas. Minerals 9 (2019) 176; doi:10.3390/min9030176

[15] J. Sampaio, A. Luz, R. Alcantera, L. Araújo, Minerais Pesados Millennium. Usinas de Beneficiamento de Minérios no Brasil; Sampaio, J.A., Luz, A.B., Lins, F.F., Eds.; Center for Mineral Technology: Rio de Janeiro, Brazil, (2001) p. 233.

[16] J. Schnellrath, M. Monte, A. Veras, H. Júnior, C. Figueiredo, Minerais Pesados INB. Usinas de Beneficiamento de Minérios no Brasil; Sampaio, J.A., Luz, A.B., Lins, F.F., Eds.; Center for Mineral Technology: Rio de Janeiro, Brazil, (2001) p. 189.

[17] S. Rosental, Terras Raras, Rochas e Minerais Industriais Usos e Especificações; Luz, A.B., Lins, F.F., Eds.; Center for Mineral Technology: Rio de Janeiro, Brazil, (2005) p. 727.

[18] T. Laxmi, S. Srikant, D. Rao, R. Rao, Beneficiation studies on recovery and in-depth characterization of ilmenite from red sediments of badlands topography of Ganjam District, Odisha, India. Int. J. Min. Sci. Technol. 23 (2013) 725–731. [CrossRef]

[19] S. Routray, R. Rao, Beneficiation and Characterization of Detrital Zircons from Beach Sand and RedSediments in India. J. Miner. Mater. Charact. Eng. 10 (2011) 1409–1428.

[20] S. Routray, T. Laxmi, R. Rao, Alternate Approaches to Recover Zinc Mineral Sand from Beach Alluvial Placer Deposits and Bandlands Topography for Industrial Applications. Int. J. Mater. Mech. Eng. 2 (2013) 80–90.

[21] E. Tranvik, M. Becker, B. Palsson, J. Franzidis, D. Bradshaw, Towards cleaner production–Using floatation to recover monazite from a heavy mineral sands zircon waste stream. Miner. Eng. 101 (2017) 30–39.

[22] M. Fawzy, Surface characterization and froth flotation of fergusonite from Abu Dob pegmatite using a combination of anionic and nonionic collectors. Physicochem. Probl. Miner. Process., 54(3) (2018) 677-687. http://dx.doi.org/10.5277/ppmp1865.

[23] M. Fawzy, Separation of fine beryl from quartz via magnetic carriers by the aiding of non-ionic surfactant Physicochem. Probl. Miner. Process., 57(2) (2021a) 14-23. DOI: 10.37190/ppmp/132329

[24] M. Fawzy, Flotation separation of dravite from phlogopite using a combination of anionic/nonionic surfactants. Physicochem. Probl. Miner. Process., 57(4) (2021b) 87-95. DOI: 10.37190/ppmp/138587

[25] EGSMA Egyptian geological survey and mining; geologic map of the Marsa Shaab, quadrangle, Egypt, scale 1:250 0000. (2002) Geol Surv Cairo, Egypt

[26] J. Rydberg J Wavelength dispersive X-ray fluorescence spectroscopy as a fast, non-destructive and cost-effective analytical method for determining the geochemical composition of small loose-powder sediment samples, J Paleolimnol 52(2014) 265–276. https:// doi. org/ 10. 1007/ s10933-014- 9792-4

[27] W-Z Zhao, B. Lu, J-B Yu, B-B Zhang, Y. Zhang, Determination of sulfur in soils and stream sediments by wavelength dispersive X-ray fluorescence spectrometry. Microchem J 156 (2020)104840. https:// doi. org/ 10. 1016/j. microc. 2020. 104840

[28] M. Zhang, B. Whiten, Determining mineral composition from assays. Proceedings of the International Heavy Mineral Conference. Australian Institute of Mining and Metallurgy, Melbourne, (2001) 81-86.

[29] R. Raju, G. Ravi, K. Shivkumar, L. Reddy, Rohatgi, WDXRFS method for quantification of heavy minerals in sand samples. Jour. GEOL. SOC. INDIA, 66 (2005) Oct. pp. 401-406.

[30] M. Rahman, M. Zaman, P. Biswas, S. Sultana, P. Nandy, Physical separation for upgradation of valuable minerals: a study on sands of the Someswari river. Bangladesh J. Sci. Ind. Res. 50(1) (2015) 53-58.

[31] Yu, Charley, Cheng, Jing-Jy, L. Jones, Y. Wang, Faillace, Ernesto, Loureiro, Celso, Y. Chia, Data collection handbook to support modeling the impacts of radioactive material in soil. (2023) 10.2172/10162250.